

## Supporting Information

### **Ring Structure Modifications of Phenylalanine 19 Increase Fibrillation Kinetics and Reduce Toxicity of Amyloid $\beta$ (1-40)**

Alexander Korn,<sup>a</sup> Dayana Surendran,<sup>b</sup> Martin Krueger,<sup>c</sup> Sudipta Maiti,<sup>b</sup> and Daniel Huster<sup>\*,a</sup>

<sup>a</sup>Institute for Medical Physics and Biophysics, Leipzig University, Härtelstr. 16-18, D-04107 Leipzig,  
Germany

<sup>b</sup>Department of Chemical Sciences, Tata Institute of Fundamental Research, Homi Bhabha Road, Colaba,  
Mumbai, 400 005, India

<sup>c</sup>Institute of Anatomy, Leipzig University, Liebigstr. 13, D-04103 Leipzig, Germany

## Materials and Methods

**Peptide synthesis.** Amyloid  $\beta$  (1-49) ( $A\beta_{40}$ ) with the primary structure DAEFRHDSGY EVHHQKL**V**FF AEDVGSNKGA IIGLMVGGVV was synthesized using standard F-moc solid phase synthesis. Residue F19 (underlined) was substituted by cyclohexyl-L-alanine (F19Cha), phenylglycine (F19-Phg), 4-phenylbutyric acid L-homophenylalanine (F19Homophe), and (1-naphthyl)-L-alanine (F19Nal); U- $^{13}\text{C}/^{15}\text{N}$  labels (Eurisotop) were introduced at positions V18, F20, A21 and G33 (bold).

**Quantum chemical calculations.** Computational amino acid modeling and quantum chemical calculations were performed using Spartan '04 windows software (Wavefunction, Inc.)

**Thioflavin T (ThT) fluorescence measurements** were used to record fibrillation kinetics. Lyophilized peptide powder was dissolved in ThT - phosphate buffer (25  $\mu\text{M}$  ThT, 25 mM sodium phosphate, 150 mM sodium chloride, 0.01% sodium azide, pH 9.2) at a concentration of 1 mg/ml. 150  $\mu\text{l}$  of the peptide solution was transferred in 96-well plates (Nunc) in triplicates, all analogs were measured in parallel on the same plate. Fluorescence was measured using a Tecan Infinite M200 Microplate Reader (Tecan Group AG, Männedorf, Switzerland) every 30 min at 37°C, with excitation at 450 nm, emission at 485 nm. The plate was shaken for 2 s every 5 min and directly before fluorescence measurements. Fluorescence intensity data were normalized by subtraction of minimum intensity value of the lag phase and division by maximum value. Using OriginPro 2017G software normalized data were fitted to a sigmoidal curve with the formula:<sup>1</sup>

$$I = y_i + m_i t + \frac{y_f + m_f t}{1 + e^{-\left[\frac{(t-t_0)}{\tau}\right]}}$$

I = intensity, t = time, m = slope,  $\tau$  = fitting parameter; fibrillation time =  $4 \times \tau$ ;  
lag time =  $t_0 - 2 \times \tau$ .

**Fibril preparation.** Lyophilized peptide powder was dissolved in alkaline phosphate buffer (25 mM sodium phosphate, 150 mM sodium chloride, 0.01% sodium azide, pH 9.2) at a concentration of 1 mg/ml

followed by dialyses with two times 400 ml phosphate buffer pH 7.4. Afterwards, the peptide solutions were transferred into reaction tubes and incubated in a thermoshaker for 7 days at 37°C and 450 rpm.

**Circular Dichroism Spectroscopy (CD)** was used to investigate secondary structure formation. A 1 mg/ml stock solution in phosphate buffer (25 mM sodium phosphate, 150 mM sodium chloride, 0.01% sodium azide, pH 7.4) was prepared and used either directly (monomers) or after 7 days of incubation at 37°C and 450 rpm (fibrils). Triplicate spectra were recorded on a Jasco J-815 CD spectrometer using 0.5 ml of a 10  $\mu$ M dilution in H<sub>2</sub>O in a 2 mm quartz cuvette.

**Transmission electron microscopy (TEM)** was used to record microscopic images and measure fibril diameters: Images were recorded by transmission electron microscopy (TEM). 2  $\mu$ l of a 1:20 dilution of fibril solution in H<sub>2</sub>O was transferred onto a formvar film-coated copper grid. After drying, the sample was stained with 1% uranyl acetate solution and images were recorded on a Zeiss SIGMA microscope equipped with a STEM detector and Atlas Software (Zeiss NTS; Oberkochen, Germany). Fibril diameters (average values, n = 100) were measured from the images using ImageJ software.

**X-ray diffraction measurements (XRD)** were performed to investigate global fibril secondary structure. Prepared fibrils were washed 3 times with H<sub>2</sub>O and high concentration fibril solution was transferred between two paraffin coated glass capillaries. After drying capillary attached fibrils were positioned in the X-ray beam of the diffractometer (Rigaku, Tokyo, Japan; X-ray source: copper rotating anode MM007 with 0.8 kW) and diffraction patterns were recorded. Spectra were extracted from the images using ImageJ software and peaks were analyzed with the OriginPro 2017G software.

**Solid-state NMR measurements** were used for local fibril structure and dynamics investigations. All NMR spectra were acquired on a Bruker 600 MHz Avance III NMR spectrometer (Bruker BioSpin GmbH, Rheinstetten, Germany) with the following setup: resonance frequency of 600.1 MHz for <sup>1</sup>H, 150.9 MHz for <sup>13</sup>C and 60.8 MHz for <sup>15</sup>N; triple channel 3.2 mm MAS probe, operation temperature 30°C. Typical pulse lengths were 4  $\mu$ s for a <sup>1</sup>H 90° pulse and 5  $\mu$ s for <sup>13</sup>C or <sup>15</sup>N 90° pulses, 1 ms <sup>1</sup>H-X CP contact time, 50 kHz spin lock field, 2.5 s relaxation delay, <sup>1</sup>H decoupling with an rf amplitude of 65 kHz using Spinal 64

decoupling.<sup>2</sup> Two dimensional NMR spectra were acquired using  $^{13}\text{C}$ - $^{13}\text{C}$  DARR and  $^{15}\text{N}$ - $^{13}\text{C}\alpha$  correlation dual acquisition experiments (during each DARR experiment eight  $^{13}\text{C}$ - $^{15}\text{N}$  correlation experiments were acquired simultaneously)<sup>3</sup> with the following parameters: 500 ms DARR mixing time, 11.777 Hz MAS frequency, 1 ms CP contact time for  $^1\text{H}$ - $^{15}\text{N}$  and 4 ms contact time for  $^{13}\text{C}$   $^{15}\text{N}$  transfer steps.  $^1\text{H}$   $^{13}\text{C}$  dipolar couplings were measured using constant time DIPSHIFT experiments<sup>4</sup> using the operation parameters: 5 kHz MAS frequency, frequency switched Lee Goldberg sequence with an effective rf field of 80 kHz for homonuclear decoupling during dipolar evolution.<sup>5</sup> Motional averaged dipolar couplings were determined from numerical simulation of the experimental dephasing curves over one rotor period.<sup>6</sup>

**3-(4,5-Dimethylthiazol-2-yl)-2,5-diphenyltetrazoliumbromid (MTT) assay** was used for quantitative cell viability measurements. Neuronal RN46A cells were seeded into 96-well plates at a density of  $1 \times 10^4$  cells/well. After 24 hours cells were treated with 100  $\mu\text{M}$  peptide solution or vehicle and incubated for 60 hours at 37°C followed by treatment with MTT solution (1 mg/ml in PBS) and incubation at 37°C for 4 hours. Precipitated formazan was dissolved with 100  $\mu\text{l}$  acidified isopropanol for 20 min under shaking on an orbital shaker. The absorbance was measured at 570 nm using a microplate reader (TECAN Infinite M200, USA) and intensity values were normalized to vehicle treated control cultures. Three independent experiments with 6 replicates each were performed.

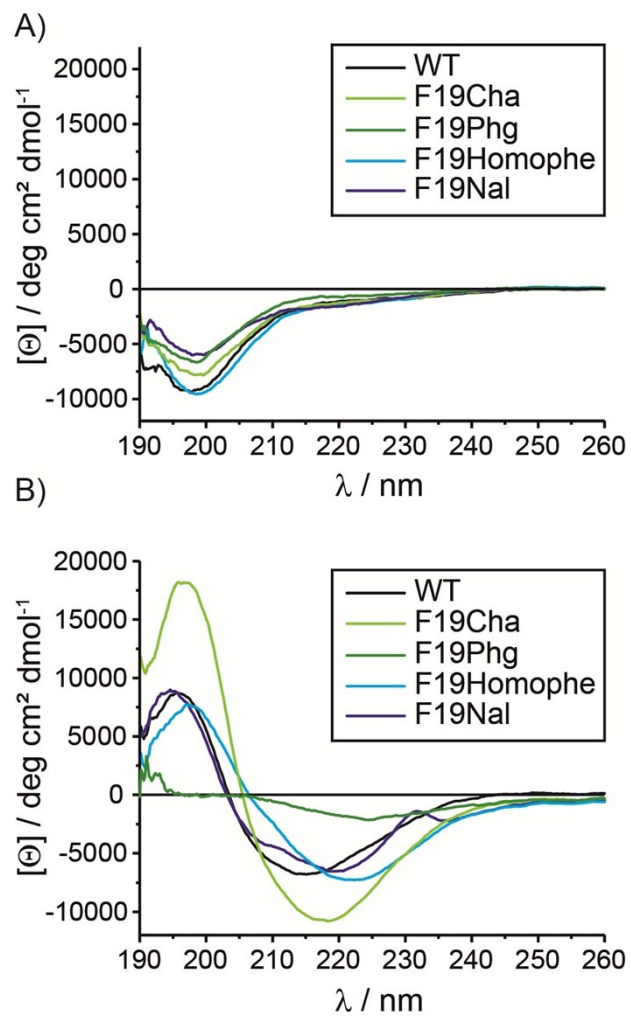


**Figure S1.** CD spectra of the  $A\beta_{40}$  peptide variants freshly prepared (A) and after an incubation period of 7 days (B).

**Table S1.** Backbone torsion angles in fibrils of mutated A $\beta_{40}$  peptides determined from the chemical shift values for V18, F19, and A21 using Talos+.<sup>7</sup>

	<b>F19</b>		<b>F20</b>		<b>A21</b>	
	$\phi / ^\circ$	$\psi / ^\circ$	$\phi / ^\circ$	$\psi / ^\circ$	$\phi / ^\circ$	$\psi / ^\circ$
WT	-110.3 $\pm$ 21.9	131.9 $\pm$ 6.9	-129.5 $\pm$ 17.8	138.2 $\pm$ 23.1	-119.2 $\pm$ 40.7	136.6 $\pm$ 24.4
F19Cha	-110.3 $\pm$ 21.9	131.9 $\pm$ 6.9	-131.0 $\pm$ 21.3	137.7 $\pm$ 16.5	-112.6 $\pm$ 41.2	144.2 $\pm$ 21.5
F19Nal	-118.7 $\pm$ 64.3	131.0 $\pm$ 19.3	-120.1 $\pm$ 22.1	126.0 $\pm$ 29.6	-109.2 $\pm$ 20.4	136.1 $\pm$ 21.3
F19Homophe	-123.5 $\pm$ 61.7	136.1 $\pm$ 21.6	-120.1 $\pm$ 22.1	126.0 $\pm$ 29.6	-108.5 $\pm$ 20.3	131.9 $\pm$ 26.0
F19Phg	-106.6 $\pm$ 26.7	135.8 $\pm$ 12.7	-109.5 $\pm$ 26.1	124.3 $\pm$ 9.8	-111.7 $\pm$ 20.8	127.4 $\pm$ 21.6

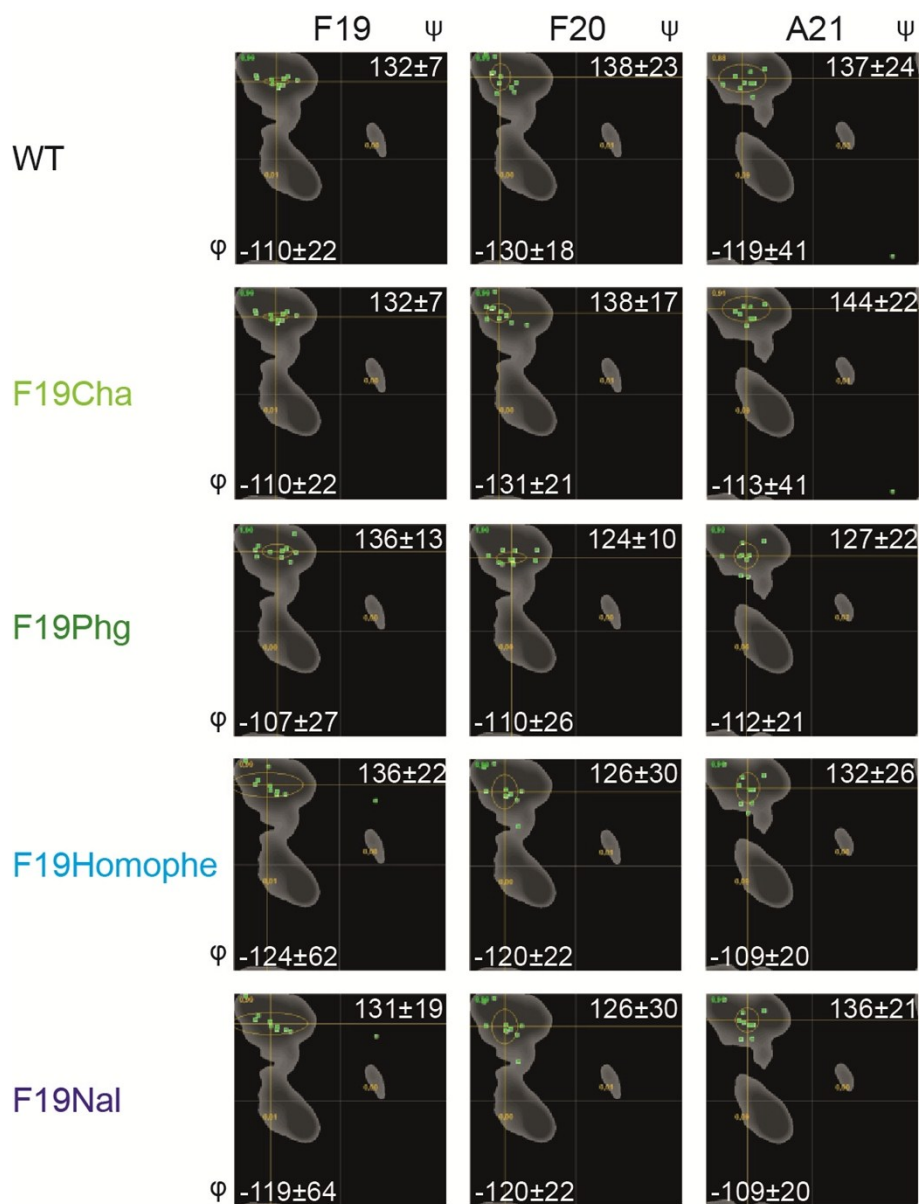


**Figure S2.** Summary of the backbone torsion angles of fibrils of mutated  $A\beta_{40}$  peptides determined from the chemical shift values for V18, F19, and A21 using Talos+ plotted as Ramachandran diagrams.<sup>7</sup>

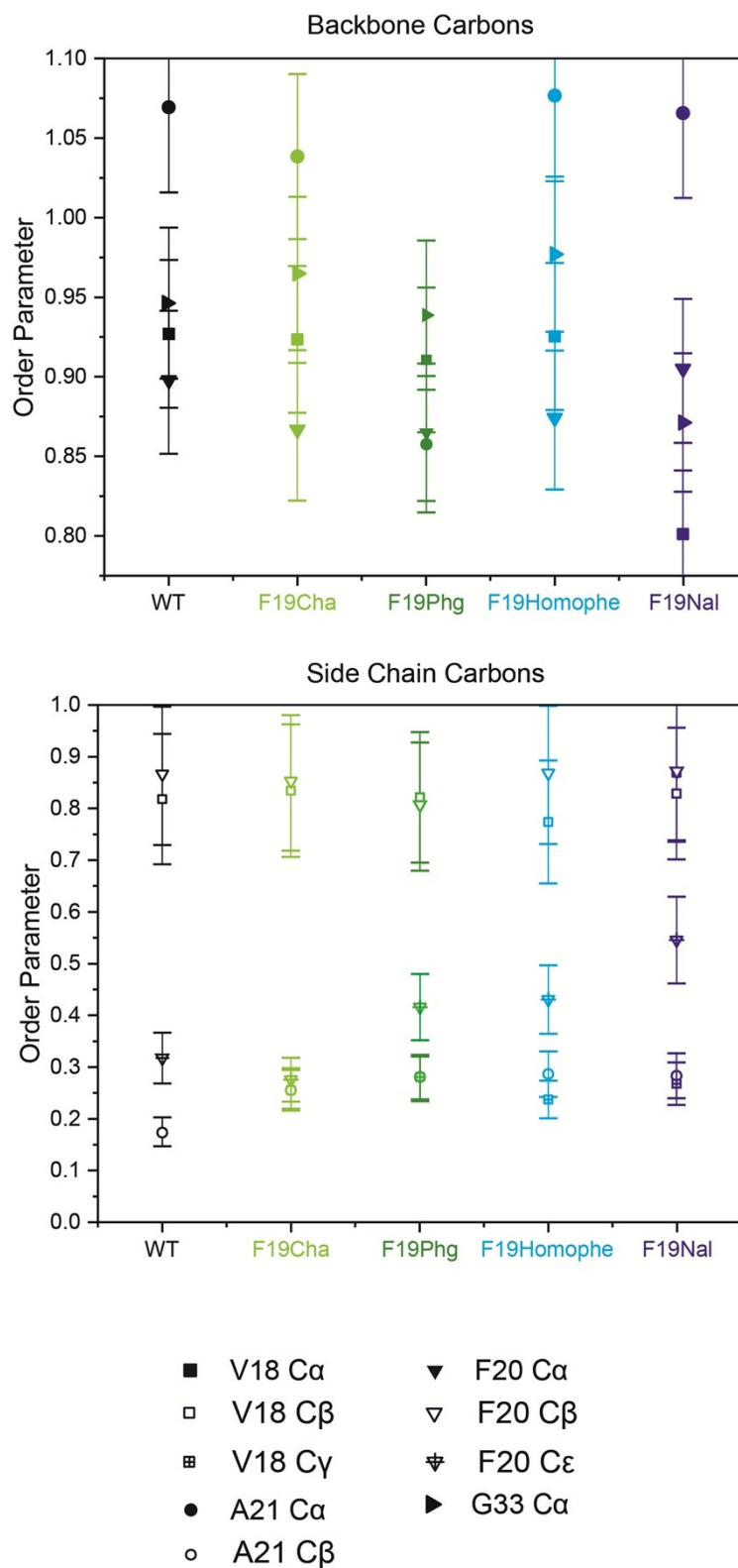


**Figure S3.**  $^1\text{H}$ - $^{13}\text{C}$  order parameters determined from fibrils of mutated  $\text{A}\beta_{40}$  peptides using DIPSHIFT experiments.



## Reference List

1. L. Nielsen, R. Khurana, A. Coats, S. Frokjaer, J. Brange, S. Vyas, V. N. Uversky, and A. L. Fink, *Biochemistry*, 2001, **40**, 6036.
2. B. M. Fung, A. K. Khitrin, and K. Ermolaev, *J. Magn Reson.*, 2000, **142**, 97.
3. T. Gopinath and G. Veglia, *Angew. Chem. Int. Ed Engl.*, 2012, **51**, 2731.
4. M. G. Munowitz, R. G. Griffin, G. Bodenhausen, and T. H. Huang, *J. Am. Chem. Soc.*, 1981, **103**, 2529.
5. A. Bielecki, A. C. Kolbert, and M. H. Levitt, *Chem. Phys. Lett.*, 1989, **155**, 341.
6. K. Schmidt-Rohr and H. W. Spiess, in *Multidimensional solid-state NMR and polymers*, Academic Press, San Diego, 1994, pp. 1.
7. Y. Shen, F. Delaglio, G. Cornilescu, and A. Bax, *J. Biomol. NMR.*, 2009, **44**, 213.